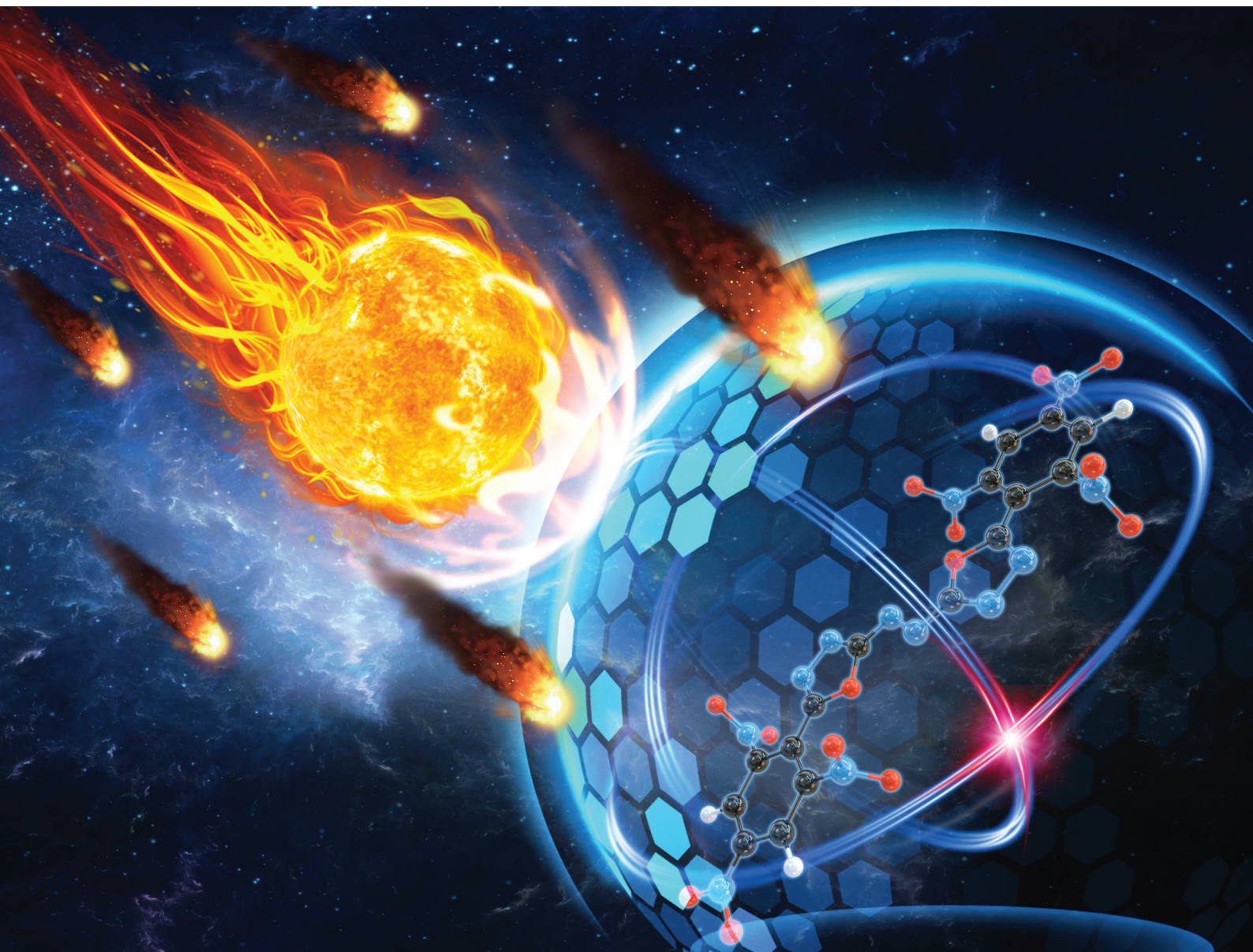


Volume 53
Number 46
14 December 2024
Pages 18387-18792

Dalton Transactions

An international journal of inorganic chemistry

rsc.li/dalton



ISSN 1477-9226



PAPER

Qiong Yu *et al.*

Energetic derivatives substituted with trinitrophenyl:
improving the sensitivity of explosives

Cite this: *Dalton Trans.*, 2024, **53**, 18467

Energetic derivatives substituted with trinitrophenyl: improving the sensitivity of explosives†

Qiong Yu,[‡] Yu-cong Chen,[‡] Zihao Guo,^a Tao Li,^a Zunqi Liu,^a Wenbin Yi,^{*a} Richard J. Staples^b and Jean'ne M. Shreeve^{b,c}

The incorporation of trinitrophenyl-modified 1,3,4-oxadiazole fragments is commonly observed in high-energy molecules with heat-resistant properties. This study explores the strategy of developing heat-resistant energetic materials by incorporating trinitrophenyl and an azo group into 1,3,4-oxadiazole, which involved the synthesis and characterization of (*E*)-1,2-bis(5-(2,4,6-trinitrophenyl)-1,3,4-oxadiazol-2-yl)diazene (**2**), *N*-(5-(2,4,6-trinitrophenyl)-1,3,4-oxadiazol-2-yl)nitramide (**3**), and the energetic salts of **3**. Characterization techniques employed included ¹H and ¹³C NMR, IR and elemental analysis. Additionally, the structures of **2** and **3** were validated using single crystal X-ray analysis. To further understand the physical and chemical characteristics of these novel energetic compounds, various calculations and measurements were performed. Compound **2** exhibits excellent thermostability (*T*_d = 294 °C), which is comparable to that of traditional heat-resistant explosive HNS (*T*_d = 318 °C). But **2** is insensitive towards impact (>40 J) and friction (>360 N), surpassing HNS (5 J, 240 N), suggesting that compound **2** deserves further investigation as a potential heat-resistant explosive.

Received 18th July 2024,
Accepted 2nd September 2024

DOI: 10.1039/d4dt02070g

rsc.li/dalton

Introduction

With the progression of time, the energetic materials utilized for national defense and civilian industries are required to meet increasingly stringent standards in terms of safety, durability, and environmental impact.^{1–3} However, traditional energetic materials fall short of meeting these requirements, both in terms of their performance and production processes. As a result, researchers from various nations have embarked on numerous challenging endeavours to design, synthesize, and develop new synthesis methods for energetic compounds, aiming to obtain high-performance explosive materials.

Among the various types of novel energetic materials currently under exploration, oxadiazole-based compounds have garnered significant attention due to their exceptional qualities such as high density, nitrogen content, and oxygen

balance. In recent years, the utilization of 1,3,4-oxadiazole as a crucial structural component in the design of energetic compounds has gained significant prominence. This is primarily attributed to its exceptional characteristics, including excellent thermal stability and low sensitivity.^{4–7} However, despite the presence of 1,3,4-oxadiazole structures, nitramines consistently exhibit inadequate thermal stabilities and sensitivities due to the inherent instability of the nitramine group. For example, the mechanical stability of the reported azo 1,3,4-oxadiazole and nitramino oxadiazoles, including bis(nitroamino-1,3,4-oxadiazole) (**ICM-101**), 2-amino-5-nitramino-1,3,4-oxadiazole (**I**) and 5-(diazo-1,2,4-triazol-3-yl)-1,3,4-oxadiazol-2-nitramino (**II**), is found to be poor. This limitation significantly restricts their potential applications (Fig. 1a).^{8–10}

Energetic materials containing trinitrophenyl typically exhibit exceptional thermal stability and low sensitivity, as seen in traditional energetic compounds such as 2,2',4,4',6,6'-hexanitrostilbene (**HNS**) and 2,5-bis-(2,4,6-trinitrophenyl)-1,3,4-oxadiazole (**DPO**).¹¹ Therefore, one effective strategy for constructing heat-resistant and insensitive explosives involves the modification of N-rich heterocycles with trinitrophenyl. This method has led to the development of highly acclaimed explosive compounds such as bis(2,4,6-trinitrophenyl) ether (**III**) and 4-amino-8-(2,4,6-trinitrophenyl)difurazano [3,4-*b*:3',4'-*e*]pyrazine (**IV**).^{12,13} These compounds serve as prominent examples of the successful application of heterocycle deriva-

^aSchool of Chemistry and Chemical Engineering, Nanjing University of Science and Technology, Nanjing 210094, China. E-mail: qyu@njust.edu.cn, yiw@njust.edu.cn^bDepartment of Chemistry, Michigan State University, East Lansing, Michigan 48824, USA^cDepartment of Chemistry, University of Idaho, Moscow, Idaho 83844-2343, USA† Electronic supplementary information (ESI) available: Experimental details for the preparation, theoretical calculations, characterization of materials. CCDC 2133005 and 2286868. For ESI and crystallographic data in CIF or other electronic format see DOI: <https://doi.org/10.1039/d4dt02070g>

‡ These authors contributed equally to this work.



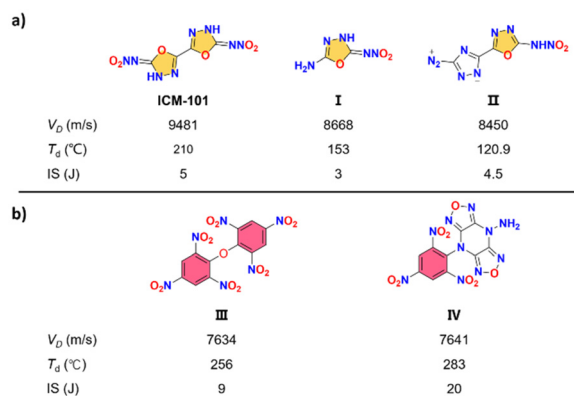


Fig. 1 Selected examples of energetic materials containing nitramino oxadiazoles (a) and trinitrophenyl (b) with their key properties.

tives in achieving the desired properties of heat resistance and insensitivity (Fig. 1b).

Considering the benefits of oxadiazole and trinitrophenyl, a strategy for combining the two to obtain energetic compounds with excellent performance is proposed. Herein, 1,3,4-oxadiazoles with azo bridged trinitrophenyl substitution (2) and 1,3,4-oxadiazoles with trinitrophenyl modified nitramine substitution (3) were synthesized for the first time. The structures of 2 and 3 were confirmed by single crystal X-ray diffraction. The single crystal data of these compounds played a crucial role in gaining a comprehensive understanding of their properties. Additionally, several analytical techniques, including Hershfield surface analysis and non-covalent interaction analysis, were employed to thoroughly characterize the molecular-level characteristics of these compounds. These meticulous analyses provided valuable insights into the properties and behaviours of compounds 2 and 3.

Results and discussion

Synthesis

All the novel compounds were synthesized starting from compound 1 which was obtained by the literature method (Fig. 2).^{11,14–17} For the synthesis of compound 2, the azo group was formed by oxidizing the amino group in compound 1 using potassium permanganate under acidic conditions. Alternatively, compound 1 was nitrated with pure nitric acid at low temperature, yielding nitrimine 3. The subsequent step involved the bubbling of excess gaseous ammonia in methanol to yield a precipitate of the ammonium salt 4. The silver salt 5 synthesized *via* metathetical reactions of silver salt 5 and hydrazine hydrochloride or hydroxylammonium chloride in methanol.

Structure analysis

The structures of compounds 2 and 3 were determined by single crystal X-ray diffraction. Detailed crystallographic data, measurement parameters, and refinement information can be

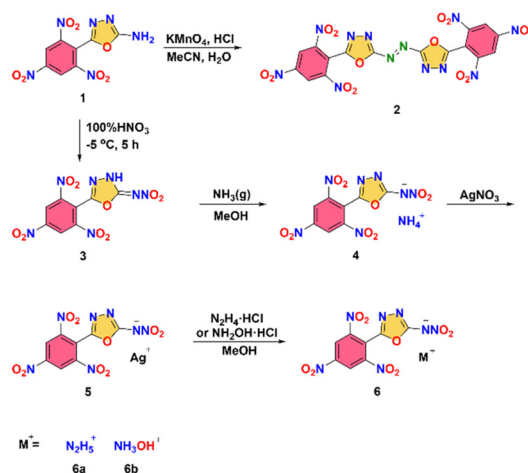


Fig. 2 Synthesis of 5-(2,4,6-trinitrophenyl)-1,3,4-oxadiazole 2-amine derivatives.

found in the Electronic ESI.† Compound 2 crystallized by the method of slow evaporation in 1,4-dioxane under yellow light at room temperature. It crystallizes in triclinic space group $P\bar{1}$ with two solvent molecules per unit cell, displaying a calculated density of 1.574 g cm^{-3} at 301.00 K (Fig. 3a). The di(1,3,4-oxadiazol-2-yl)diazene is coplanar, but it is twisted out of the plane formed by the 2,4,6-trinitrophenyl functionalities with an angle of $94.0(3)^\circ$. The two picryl groups are aligned in a parallel manner. Interestingly, two nitro groups attached to C8 and C10 exhibit significant bending out of the benzene

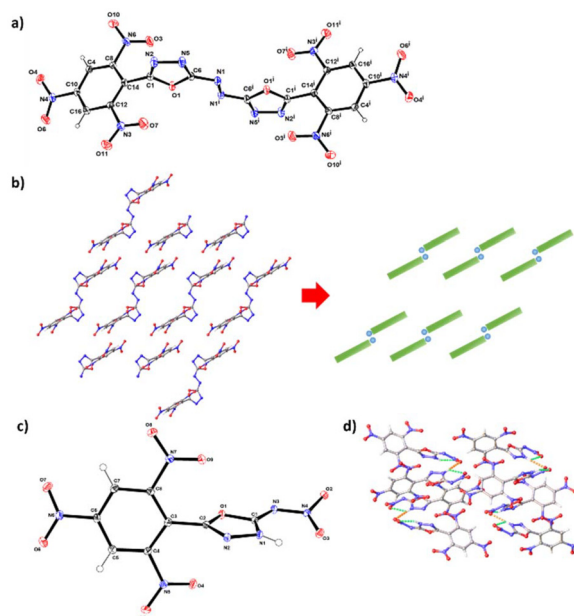


Fig. 3 (a) Molecular structure of 2, cocrystallized solvent molecules were removed for clarity; (b) ball & stick packing diagram of 2, cocrystallized solvent molecules are removed for clarity; (c) molecular structure of 3; (d) ball & stick packing diagram of 3 with intramolecular (green) and intermolecular (orange) hydrogen bond interactions.



ring plane, with torsion angles measured as O4–N4–C10–C4 at 21.8(3)° and O3–N6–C8–C14 at 21.6(4)°. However, one nitro group attached to the atom C12 shows a slight twisting (O1–N3–C12–C16 at 7.3(4)°). Due to the presence of azo bridges, compound **2** features a Z-shaped structure with embedded stacking structures (Fig. 3b), which makes it insensitive to impact and friction. This structural setup allows for the absorption of mechanical forces by converting them into intermolecular interaction energy. This process helps prevent excessive molecular vibration, thereby reducing the risk of explosive decomposition, hot spot formation, and eventual detonation.

Compound **3** adopts a monoclinic crystal structure in the space group *Pbca* with a crystal density of 1.865 g cm⁻³ at 100 K (Fig. 3c). It is noteworthy that each unit cell contains 8 molecules. The trinitrobenzene ring and the oxadiazole ring display a twisted conformation, with a dihedral angle of 79.67° as evidenced by the torsion angles of O1–C2–C3–C8 (–81.06 (15)°) and N2–C2–C3–C8 (101.41(17)°). There are both intramolecular and intermolecular hydrogen bonds were observed in compound **3**, with bond lengths of approximately 2.2 Å and 2.1 Å, respectively. The presence of these strong hydrogen bonds significantly contributes to the enhancement of molecular stability.

Performance

In order to investigate the potential application prospects of the energetic compounds which have been synthesized, a number of physicochemical properties have been determined and are given in Table 1. The densities of compounds **1**, **2**, **3**, **4**, **6a** and **6b** were experimentally measured using a gas pycnometer under a helium atmosphere at 25 °C. To ensure accuracy, three measurements were conducted for each compound, and the average values are presented in Table 1. The densities of all compounds range from 1.76 to 1.80 g cm⁻³. In particular, the measured density of compound **2** without solvent is 1.79 g cm⁻³, surpassing that of HNS. Another crucial property to consider when designing energetic materials is the heat of formation (ΔH_f), which was calculated using Gaussian 16 program.¹⁸ Compounds **2** and **3** exhibit high positive ΔH_f values of 666.6 and 256.5 kJ mol⁻¹, respectively, surpassing the value of HNS. The presence of azo bonds leads to a higher

enthalpy of formation for compound **2** compared to 5,5'-bis(2,4,6-trinitrophenyl)-2,2'-bi(1,3,4-oxadiazole) (TKX-55), but it has a lower density than TKX-55. Utilizing the experimental density and calculated ΔH_f , the detonation velocity (V_D) and detonation pressure (P) were evaluated using EXPLO-5 software (version 6.01).¹⁹ The detonation velocity of **2** exceeds those of HNS¹¹ and TNT²⁰. Thermal stability evaluations of all compounds were conducted using differential scanning calorimetry under a nitrogen atmosphere with a heating rate of 5 °C min⁻¹. The decomposed temperature of compound **2** demonstrates similarity to that of HNS, indicating its potential suitability as a heat-resistant explosive. After oxidation of the amino group in compound **1** to form **2**, the heat of formation of the compound greatly increases, and the density also slightly increases, which leads to an increase in the energy density of the compound.

The sensitivities of all compounds to impact and friction were assessed by a standard BAM drop hammer apparatus and BAM friction tester. As indicated in Table 1, with the exception of **3**, all the other compounds demonstrate high insensitivity to both impact and friction. However, compound **3** is much more insensitive than the reported nitramines. Compound **2** demonstrates favourable impact sensitivity above 40 J and friction sensitivity exceeding 360 N, surpassing those of traditional heat-resistant explosive HNS. The impact sensitivity of compound **2** also exceeds that of TKX-55 (IS = 5 J).

In order to understand the correlation regarding these innovative materials and their physical characteristics, a comparison was made between the Hirshfeld surface, two-dimensional fingerprints, and the proportional contributions of close contacts for compounds **2** and **3**. This analysis is illustrated in Fig. 4.

The Hirshfeld surfaces and corresponding two-dimensional (2D) fingerprints of **2** and **3** in their crystal structures were analysed to explore the connection between intermolecular interactions and physical properties.²¹ The effects of the Hirshfeld surfaces were processed by colour codes, with red spots representing regions of intense intermolecular interactions. Regular 2D fingerprints reveal the presence of diverse interactions originating from various sources. From the 2D fingerprints of compounds **2** and **3**, it was observed that there are limited highly

Table 1 Physicochemical properties of **1**, **2**, **3**, **4**, **6a**, **6b**, TKX-55, HNS and TNT

Compound	T_{dec}^a [°C]	ρ^b [g cm ⁻³]	ΔH_f^c [kJ mol ⁻¹]	V_D^d [m s ⁻¹]	P^e [GPa]	IS ^f [J]	FS ^g [N]
1	231	1.76	155.0	7447	22.6	>40	>360
2	294	1.79	666.6	7763	25.3	>40	>360
3	144	1.79	222.6	8075	27.9	20	160
4	188	1.80	–625.7	7193	20.1	>40	240
6a	145	1.78	–464.6	7366	21.5	>40	160
6b	151	1.78	–557.1	7394	22.0	>40	160
TKX-55 ^h	335	1.84	197.6	8030	27.3	5	>360
HNS ^h	318	1.74	78.2	7612	26.3	5	240
TNT ⁱ	295	1.65	–67	6809	18.7	15	353

^a Onset decomposition temperature from DSC (5 °C min⁻¹). ^b Density at 298 K. ^c Heat of detonation. ^d Detonation velocity: EXPLO5_V6.01. ^e Detonation pressure: EXPLO5_V6.01. ^f IS: impact sensitivity. ^g FS: friction sensitivity. ^h Ref. 11. ⁱ Ref. 20.



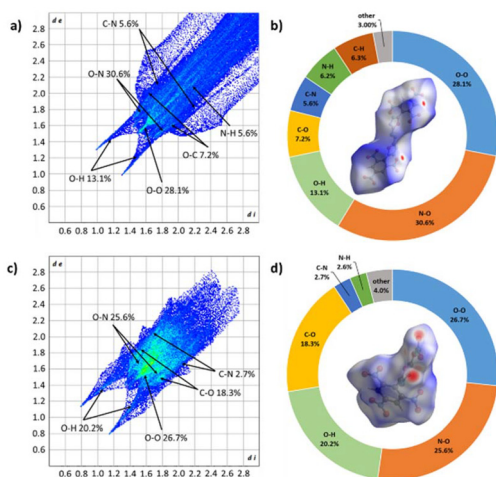


Fig. 4 Hirshfeld surfaces and 2D fingerprint plots in crystal stacking for 2 (a and b) and 3 (c and d).

unstable O–O interactions leading to high instability in the compound. Additionally, a small amount of C–N interaction, indicative of π – π interactions, contributes to lower mechanical sensitivity. In the case of compound 3, the 2D fingerprint also showed O–H interactions, suggesting a significant presence of hydrogen bonds in the compound, which contributes to its lower impact and friction.



Fig. 6 Structural comparison between compound 2 and TKX-55.

Typically, the aromaticity of molecules is considered a critical determinant of their thermal stability.²² Consequently, the molecular aromaticity of compounds 2 and 3 was investigated by generating associated ICSSs using Multiwfn v4.5 software (Fig. 5).²³ The benzene and 1,3,4-oxadiazole rings in compounds 2 and 3 exhibit significant strong aromaticity with each ring being distinctly shielded. This characteristic contributes to the stability of compounds 2 and 3. The azo bond in compound 2 serves as a bridge linking two oxadiazole rings, creating a substantial conjugated system that boosts the compound's aromaticity. In contrast, the two oxadiazole rings in TKX-55 are directly linked by C–C bonds, rendering compound 2 more resistant to impact than TKX-55 (Fig. 6).

Conclusions

To summarize, we have presented an effective method for synthesizing azo compounds 2, nitrimine 3, and their high-energy salts 4, 6a, and 6b derived from 5-(2,4,6-trinitrophenyl)-1,3,4-oxadiazole 2-amine (1). Compound 2 demonstrates remarkable thermal stability, characterized by a decomposition temperature (T_d) of 294 °C. Moreover, it exhibits extremely low mechanical sensitivity, superior to the performance of HNS, suggesting its potential use in heat-resistant explosives. Compound 3 exhibits trinitrophenyl and profound hydrogen bonding interactions both intramolecularly and intermolecularly, resulting in stable structure and insensitivity (IS = 20 J and FS = 160 N). Utilizing ICSS and Hirshfeld surfaces to investigate the factors leading to the lower sensitivity of compounds 2 and 3 in comparison to similar compounds. The presence of trinitrophenyl markedly enhances the heat resistance and mechanical sensitivity of the compounds. These discoveries pave the way for future synthesis of heat-resistant and insensitive derivatives of 1,3,4-oxadiazole compounds.

Experimental section

Caution! In this work, some compounds are potential high-energy materials and are prone to explode under certain external stimuli. Certain compounds require preparation at high temperatures. Therefore, the entire experimental process

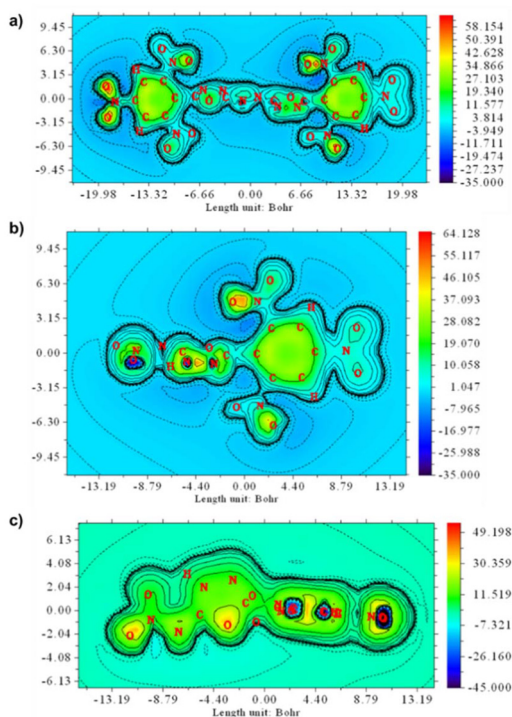


Fig. 5 (a) Shielding map of compound 2, (b) Shielding map of compound 3 benzene plane, (c) Shielding map of compound 3 oxadiazole plane.



should be conducted using appropriate safety equipment such as safety hoods, goggles, and leather gloves. Mechanical actions involving scraping, impacting, or scratching must be avoided. Additionally, some hazardous compounds must be synthesized on a small scale.

General methods

The reagents were purchased from Admas, Acros Organics and Aldrich and used directly without any additional treatment. ^1H NMR and ^{13}C NMR spectra were recorded by Bruker AVANCE 300 and AVANCE III 500 MHz, operating at 300 (500) and 75 MHz, respectively. d_6 -DMSO was used as a solvent and for field locking. Chemical shifts are reported relative to $(\text{CH}_3)_4\text{Si}$ in the ^1H and ^{13}C spectra. The decomposition (onset temperature) points were obtained using a differential scanning calorimeter. The decomposition (onset temperature) points were measured using a differential scanning calorimeter (TA Instruments Co., model Q2000) at a heating rate of $5\text{ }^\circ\text{C min}^{-1}$. Elemental analyses of C/H/N were performed on a Vario Micro cube Elementar Analyser.

Synthesis of (*E*)-1,2-bis(5-(2,4,6-trinitrophenyl)-1,3,4-oxadiazol-2-yl)diazene (2)

5-(2,4,6-Trinitrophenyl)-1,3,4-oxadiazol-2-amine (**1**) (0.592 g, 2.0 mmol) was added to a mixture of concentrated hydrochloric acid (7 mL) and acetonitrile (6 mL). KMnO_4 (0.379 g, 2.4 mmol) was dissolved in water (15 mL) and added dropwise to the reaction mixture. The reaction was carried out at room temperature for 2 hours. The reaction mixture was treated with 30% hydrogen peroxide until the black disappears and turns pale yellow. The precipitate was collected by filtration, washed with water (10 mL), and dried under vacuum to give 0.371 g (63.1%) of **2** as a pale yellow solid.

T_d (onset): $294\text{ }^\circ\text{C}$. ^1H NMR (d_6 -DMSO): $\delta = 9.39$ (s, 4H) ppm; ^{13}C NMR (d_6 -DMSO): $\delta = 168.7, 157.5, 150.2, 149.2, 125.2, 116.9$ ppm; IR (KBr pellet): 3113, 3085, 2917, 2884, 1610, 1549, 1343, 1250, 1183, 1111, 1075, 1026, 979, 925, 739, 724 cm^{-1} ; elemental analysis (%) calcd for $\text{C}_{16}\text{H}_4\text{N}_{12}\text{O}_{14}$ (588.0): C, 32.67; H, 0.69; N, 28.57; O, 38.07; found: C, 32.95; H, 0.87; N, 27.43; O, 38.75.

Synthesis of *N*-(5-(2,4,6-trinitrophenyl)-1,3,4-oxadiazol-2-yl)nitramide (3)

5-(2,4,6-Trinitrophenyl)-1,3,4-oxadiazol-2-amine (**1**) (0.592 g, 2.0 mmol) was added in small batches to 100% nitric acid (2 mL) at $-5\text{ }^\circ\text{C}$ and maintained the same temperature for 5 hours. Then the reaction mixture was poured onto 10 g of ice. Yellow solid was collected from the solution through filtration, washed with water and dichloromethane and dried under vacuum to leave a yellow solid (0.493 g, 72.3% yield).

T_d (onset): $144\text{ }^\circ\text{C}$. ^1H NMR (CD_3CN): $\delta = 9.30$ (s, 2H) ppm; ^{13}C NMR(CD_3CN): $\delta = 163.4, 151.9, 151.3, 149.7, 126.4, 126.3$ ppm; IR (KBr pellet): 3423, 3088, 2921, 1656, 1592, 1556, 1488, 1338, 1276, 1085, 1065, 979, 921, 826, 782, 748, 725, 690 cm^{-1} ; elemental analysis (%) calcd for $\text{C}_8\text{H}_3\text{N}_7\text{O}_9$ (341.0):

C, 28.17; H, 0.89; N, 28.74; O, 42.21; found: C, 28.47; H, 1.04; N, 27.98; O, 42.51.

Synthesis of ammonium nitro(5-(2,4,6-trinitrophenyl)-1,3,4-oxadiazol-2-yl)amide (4)

NH_3 gas was slowly bubbled into a solution of compound **3** (0.682 g 2 mmol) in MeOH (6 mL), being stopped when mixture pH = 7. The precipitate was filtered, and dried to obtain yellow solid with a yield of 63% (0.451 g).

T_d (onset): $188\text{ }^\circ\text{C}$. ^1H NMR (d_6 -DMSO): $\delta = 9.24$ (s, 2H), 7.10 (s, 4H) ppm; ^{13}C NMR (d_6 -DMSO): $\delta = 167.3, 149.03, 148.99, 148.9, 123.9, 118.1$ ppm; IR (KBr pellet): 3438, 3162, 3100, 1608, 1541, 1406, 1343, 1184, 1112, 1047, 916, 783, 759, 743, 724, 609 cm^{-1} ; elemental analysis (%) calcd for $\text{C}_8\text{H}_6\text{N}_8\text{O}_9$ (358.0): C, 26.83; H, 1.69; N, 31.28; O, 42.20; found: C, 27.09; H, 1.91; N, 30.55; O, 40.45.

Synthesis of silver nitro(5-(2,4,6-trinitrophenyl)-1,3,4-oxadiazol-2-yl)amide (5)

Under stirring, the solution of AgNO_3 (0.169 g, 1 mmol) in H_2O (2 mL) was added dropwise to the solution of compound **4** (0.358 g, 1 mmol) in H_2O . After two hours, the precipitate was filtered, and dried to obtain yellow solid with a yield of 93% (0.417 g).

T_d (onset): $277\text{ }^\circ\text{C}$. ^1H NMR (d_6 -DMSO): $\delta = 9.27$ (s, 2H) ppm; ^{13}C NMR (d_6 -DMSO): $\delta = 168.7, 151.0, 150.9, 150.6, 125.9, 119.5$ ppm; IR (KBr pellet): 3438, 3067, 2890, 1606, 1541, 1463, 1340, 1291, 1176, 1089, 988, 979, 784, 771, 760, 744, 724 cm^{-1} ; elemental analysis (%) calcd for $\text{C}_8\text{H}_6\text{N}_8\text{O}_{10}$ (446.9): C, 21.45; H, 0.45; N, 21.89; O, 32.14; found: C, 21.69; H, 0.691; N, 20.69; O, 56.93.

General procedure for synthesis of salts 6

Monohydrochloride hydrazine (1 mmol), or hydroxylammonium chloride (1 mmol) was added to a suspension of **5** (1 mmol) in methanol (20 mL). After stirring the mixture at ambient temperature for 2 hours, the silver chloride was removed by filtration and washed with a small amount of methanol. The methanol was removed under vacuum to obtain salts **6**.

Hydrazinium nitro(5-(2,4,6-trinitrophenyl)-1,3,4-oxadiazol-2-yl)amide (6a)

Yellow solid (0.3335 g, 90%); T_d (onset): $145\text{ }^\circ\text{C}$. ^1H NMR (d_6 -DMSO): $\delta = 9.27$ (s, 2H) 7.21 (s, 5H) ppm; ^{13}C NMR(d_6 -DMSO): $\delta = 167.2, 149.0, 148.9, 124.1, 123.9, 118.1$ ppm; IR (KBr pellet): 3433, 3221, 3092, 2967, 1607, 1581, 1545, 1408, 1345, 1312, 1191, 1063, 999, 924, 780, 735, 725 cm^{-1} ; elemental analysis (%) calcd for $\text{C}_8\text{H}_7\text{N}_9\text{O}_9$ (373.0): C, 25.75; H, 1.89; N, 33.78; O, 38.58; found: C, 26.08; H, 2.23; N, 31.61; O, 40.08.

Hydroxylammonium nitro(5-(2,4,6-trinitrophenyl)-1,3,4-oxadiazol-2-yl)amide (6b)

Yellow solid (0.322 g, 86%); T_d (onset): $151\text{ }^\circ\text{C}$. ^1H NMR (d_6 -DMSO): $\delta = 10.12$ (s, 4H) 9.25 (s, 2H) ppm; ^{13}C NMR(d_6 -DMSO): $\delta = 167.0, 149.2, 149.1, 149.0, 124.1, 118.1$ ppm; IR



(KBr pellet): $\tilde{\nu} = 3449, 3223, 3092, 2735, 1607, 1545, 1408, 1345, 1192, 1064, 981, 924, 780, 735, 725 \text{ cm}^{-1}$; elemental analysis (%) calcd for $\text{C}_8\text{H}_6\text{N}_8\text{O}_{10}$ (374.2): C, 25.68; H, 1.62; N, 29.95; O, 42.76; found: C, 25.94; H, 1.93; N, 27.81; O, 44.32.

Data availability

All information concerning the synthesis and properties of the newly synthesized materials is included in the manuscript or the ESI.†

Conflicts of interest

The authors declare that they have no known competing financial interests or personal relationships that could have appeared to influence the work reported in this paper.

Acknowledgements

We would like to express our gratitude to the National Natural Science Foundation of China (22305124), and the Natural Science Foundation of Jiangsu Province (BK20220967).

References

- G. Bélanger-Chabot, M. Rahm, R. Haiges and K. O. Christe, *Angew. Chem., Int. Ed.*, 2015, **54**, 11730–11734.
- J. Zhang, Q. Zhang, T. T. Vo, D. A. Parrish and J. M. Shreeve, *J. Am. Chem. Soc.*, 2015, **137**, 1697–1704.
- H. Li, L. Zhang, N. Petrutik, K. Wang, Q. Ma, D. Shem-Tov, F. Zhao and M. Gozin, *ACS Cent. Sci.*, 2020, **6**, 54–75.
- T. S. Hermann, K. Karaghiosoff, T. M. Klapötke and J. Stierstorfer, *Chem. – Eur. J.*, 2017, **23**, 12087–12091.
- Y. Du, Z. Qu, H. Wang, H. Cui and X. Wang, *Propellants, Explos., Pyrotech.*, 2021, **46**, 860–874.
- S. Banik, P. Kumar, V. Ghule, S. Khanna, D. Allimuthu and S. Dharavath, *J. Mater. Chem. A*, 2022, **10**, 22803–22811.
- A. K. Yadav, V. D. Ghule and S. Dharavath, *ACS Appl. Mater. Interfaces*, 2022, **14**, 49898–49908.
- W. Zhang, J. Zhang, M. Deng, X. Qi, F. Nie and Q. Zhang, *Nat. Commun.*, 2017, **8**, 181.
- Q. Sun, N. Ding, C. Zhao, J. Ji, S. Li and S. Pang, *Chem. Eng. J.*, 2022, **427**, 130912.
- Z. Dong, Z. Wu, Q. Zhang, Y. Xu and G. Lu, *Front. Chem.*, 2022, **10**, 996812.
- T. M. Klapötke and T. G. Witkowski, *Chempluschem*, 2016, **81**, 357.
- M. Reichel, D. Dosch, T. M. Klapötke and K. Karaghiosoff, *J. Am. Chem. Soc.*, 2018, **141**, 1911–1916.
- N. Liu, Y. Shu, H. Li, L. Zhai, Y. Li and B. Wang, *RSC Adv.*, 2015, **5**, 43780–43785.
- Z. Yao, R. Wang and H. Liu, *Appl. Chem. Ind.*, 2009, **38**, 1153–1155.
- T. Huang, B. Jin, R. Peng and S. Chu, *Int. J. Polym. Anal. Charact.*, 2014, **19**, 522–531.
- G. P. Sharnin, B. I. Buzykin and R. K. Fassakhov, *Chem. Heterocycl. Compd.*, 1977, **13**, 598–601.
- T. K. Shkinyova, I. L. Dalinger, S. I. Molotov and S. A. Shevelev, *Russ. Chem. Bull.*, 2000, **49**, 1572–1574.
- M. J. Frisch, G. W. Trucks, H. B. Schlegel, G. E. Scuseria, M. A. Robb, J. R. Cheeseman, G. Scalmani, V. Barone, G. A. Petersson, H. Nakatsuji, X. Li, M. Caricato, A. V. Marenich, J. Bloino, B. G. Janesko, R. Gomperts, B. Mennucci, H. P. Hratchian, J. V. Ortiz, A. F. Izmaylov, J. L. Sonnenberg, D. Williams, F. Ding, F. Lipparini, F. Egidi, J. Goings, B. Peng, A. Petrone, T. Henderson, D. Ranasinghe, V. G. Zakrzewski, J. Gao, N. Rega, G. Zheng, W. Liang, M. Hada, M. Ehara, K. Toyota, R. Fukuda, J. Hasegawa, M. Ishida, T. Nakajima, Y. Honda, O. Kitao, H. Nakai, T. Vreven, K. Throssell, J. A. Montgomery Jr., J. E. Peralta, F. Ogliaro, M. J. Bearpark, J. J. Heyd, E. N. Brothers, K. N. Kudin, V. N. Staroverov, T. A. Keith, R. Kobayashi, J. Normand, K. Raghavachari, A. P. Rendell, J. C. Burant, S. S. Iyengar, J. Tomasi, M. Cossi, J. M. Millam, M. Klene, C. Adamo, R. Cammi, J. W. Ochterski, R. L. Martin, K. Morokuma, O. Farka, J. B. Foresman and D. J. Fox, *Gaussian 16, Revision A.03*, Wallingford, CT, 2016.
- M. Sućeska, *EXPLO5 6.05*, Brodarski Institute, Zagreb, Croatia, 2020.
- Y. Li, P. Chen, Y. Liu, P. Yin, C. He and S. Pang, *Chin. J. Chem.*, 2020, **38**, 1619–1624.
- M. J. Turner, J. J. McKinnon, S. K. Wolff, D. J. Grimwood, P. R. Spackman, D. Jayatilaka and M. A. Spackman, *Crystal Explorer (Version 17.5)*, University of Western Australia, 2017.
- Z. Chen, C. S. Wannere, C. Corminboeuf, R. Puchta and P. v. R. Schleyer, *Chem. Rev.*, 2005, **105**, 3842–3888.
- T. Lu and F. Chen, *J. Comput. Chem.*, 2012, **33**, 580–592.

